

International Journal of Pavement Engineering



ISSN: 1029-8436 (Print) 1477-268X (Online) Journal homepage: https://www.tandfonline.com/loi/gpav20

An investigation towards intelligent tyres using finite element analysis

Pooya Behroozinia, Seyedmeysam Khaleghian, Saied Taheri & Reza Mirzaeifar

To cite this article: Pooya Behroozinia, Seyedmeysam Khaleghian, Saied Taheri & Reza Mirzaeifar (2020) An investigation towards intelligent tyres using finite element analysis, International Journal of Pavement Engineering, 21:3, 311-321, DOI: 10.1080/10298436.2018.1475664

To link to this article: https://doi.org/10.1080/10298436.2018.1475664

	Published online: 24 May 2018.
	Submit your article to this journal 🗷
ılıl	Article views: 127
Q ^L	View related articles ☑
CrossMark	View Crossmark data ☑
4	Citing articles: 1 View citing articles 🗗





An investigation towards intelligent tyres using finite element analysis

Pooya Behroozinia^{a,b}, Seyedmeysam Khaleghian^a, Saied Taheri^a and Reza Mirzaeifar^a

^aDepartment of Mechanical Engineering, Virginia Tech, Blacksburg, VA, USA; ^bMaxxis Technology Center, Suwanee, GA, USA

ABSTRACT

Intelligent tyres have the potential to be widely used to enhance the safety of road transportation systems by providing an estimation of the road surface friction, tyre load and several other important characteristics. Since the tyre–road contact characteristics play an important role in stability and control of vehicles under severe manoeuvers, tyre interaction with the road surface needs to be evaluated in the contact patch region. In this research, a finite element model is implemented to investigate the effects of different parameters, including vehicle velocity and normal load, on the projected contact patch area. Furthermore, a tyre with a tri-axial accelerometer attached to its inner-liner is tested on different road surfaces with different contact frictions and at different loading conditions. To validate the model, the radial and circumferential accelerations obtained from the simulation are compared with the experimental results. The effects of velocity, normal load and coefficient of friction on the contact patch area are investigated and it is concluded that the circumferential component of acceleration is the key factor for estimating the tyre contact patch length.

ARTICLE HISTORY

Received 28 November 2016 Accepted 4 May 2018

KEYWORDS

Intelligent tyre; finite element method; tyre contact patch length; tyre– road friction

1. Introduction

Tyres play one of the most important roles in the vehicles performance, since they are the only parts of the vehicle which are in contact with the road surface. Monitoring the interaction between the tyre and the road can result in extraction of valuable tyre–road contact information that can be used to improve the performance of ABS and stability controllers. Different sensors are used inside the tyre to monitor the tyre–road interaction, and to estimate the deflection of tread elements inside the contact patch (Khaleghian *et al.* 2017).

The sensor types are mostly accelerometer, piezoelectric and magnetic sensors. Erdogan et al. (2011a) used piezoelectric sensors inside the tyre (in tread area) to estimate the lateral deflection profile of the carcase and utilised it to estimate the friction. Magnets vulcanised into the tread of a Kevlar-belted tyre are also used in some studies to measure the deflection of the tread in x, y and z directions as a function of its position inside the contact patch (Breuer 1992, Eichhorn and Roth 1992, Bachmann 1995, Breuer et al. 2000, Hollingum 2001). Using the fact that the tread deformation is caused by the total force acting on the tyre, the friction is estimated. In other studies, tri-axial accelerometers attached to the inner-liner of the tyre are used to estimate the friction (Singh et al. 2013). Matilainen and Tuononen (2011, 2012) used the signals from a tri-axial accelerometer inside the tyre to estimate contact patch length. The algorithm detects two acceleration peaks in the longitudinal acceleration signal and uses it along with wheel angular speed to estimate contact patch. Khaleghian et al. (2016, Khaleghian and Taheri 2017) and Singh et al. (2013) utilised a tri-axial accelerometer attached to the inner-liner of the tyre and developed a neural network algorithm to estimate the tyre normal load. Niskanen and Tuononen (2014a, 2014b, 2015) used

three tri-axial accelerometers inside the tyre to find friction indicators on smooth ice and concrete surfaces. The radial acceleration signal from the accelerometer is analysed at the leading edge of the contact patch for friction indicators. They have stated that the vibration in the leading edge due to slip on low friction surfaces can be used to determine the road surface type.

Developing a comprehensive intelligent tyre-based algorithms is an expensive and time consuming process; experimental data with different velocities, tyre pressure, various loading and road conditions should be used to train the algorithm. Finite element method (FEM) is a powerful tool that is widely used in the tyre as well as other industries to reduce the time and cost of experimental process. Hence, in order to train the intelligent tyre-based algorithms, developing the FE intelligent tyre models is more efficient than conducting experiments. In addition, finite element (FE) models can represent the tyre/ ground interaction (Zang et al. 2011, Wang et al. 2013). Xia and Yang (2012) presented a 3D FE model for tyre/ground interaction and used hyperelastic material properties for rubber in their analysis. Dynamic analysis was employed in order to predict the dynamic ground response due to moving vehicle. Moreover, the interaction of different tyres (used on heavy and light vehicles) with pavement was analysed in the literature and their works were validated by the static test data (Cao et al. 2015, Cao et al. 2016). Kennedy and Padovan (1987) developed a formulation in FEM to analyse the radial automobile tyres rotating with a steady-state velocity. They considered the dynamic problem requiring solution in the time domain as a quasi-static problem using static analysis solution by changing the time derivatives to spatial derivatives. Hence, the computational time was reduced by their special formulations and

their study was the first three dimensional model of a tyre rotating with a steady-state velocity. In the literature, FEM results of rolling tyres are generally compared with experimental data collected using the flat-track tyre testing machines (Tönük and Ünlüsoy 2001, Gent and Walter 2006). However, the large flat surface testing machines are expensive, require large laboratory space and conducting experiments is very time consuming. Korunović et al. (2011) presented a flexible CAD-based meshing approach in the FE modelling of a tyre rolling on the drum in order to help tyre designers find the optimal values of tyre design parameters quickly. They implemented braking and cornering tests to compare their numerical results with the experimental data. The friction between the drum and the tyre defined by Coulomb model with viscous stick equations was calibrated to improve their model.

In addition to steady-state analysis of tyre, FEM can be utilised to evaluate the dynamic response of tyres using explicit time integration techniques (Kao and Muthukrishnan 1997). The transient analysis of impact problems are widely solved by explicit FEM. Koishi et al. (1998) computed the cornering force of tyres using an explicit FEM code and compared their results with the experimental ones implemented by MTS Flat-Track tyre test system. Using explicit FEM, Cho et al. (2005) modelled the impact of a rolling tyre with a small cleat. They obtained the frictional dynamic contact equations using the Lagrangian and Penalty methods. They demonstrated the effects of rolling speed and inflation pressure on the transient dynamic response of tyres. The life prediction of rolling tyres computed by the FEM linked with failure criteria is another advantage of using numerical analysis in tyre mechanics. Extended finite element method (XFEM) (Behroozinia et al. 2016a) and sub-modelling techniques (Han et al. 2004) are the tools for predicting the damage propagation in structures. Using FEM, Ebbott (1996) calculated the energy release rate of a crack in a local model obtained from a global tyre model by using Virtual Crack Closure Technique. Erdogan et al. (2011b) used a tyre FE model to generate lateral, tangential and radial tyre accelerations for a fixed load and slip angle. The effects of normal load, tyre pressure and vehicle velocity on the acceleration signals were investigated.

Vertical and shear contact pressure distributions on tyres and pavements are affected by tyre inflation pressure and normal load. The effect of tyre configuration on the pavement performance has been studied using the 3D FE modelling. De Beer et al. (2012) developed several tyre models in order to show different important factors, required to be considered in the road pavement design. Four tyre models were developed in order to present the effect of tyre modelling on the road pavement response, since the contact stress distribution changed with different normal loads and inflation pressures applied to the tyre models. Zhao and Zang (2014) developed a 3D simulation to study the tyre/ sand interaction by coupling finite discrete element and FEMs. They presented a new algorithm for the contact estimation and validated their work by comparing the numerical results with experiments. Wang et al. (2012) developed a 3D FE model of tyre/pavement interaction to predict the contact stress distribution in the contact patch surface. The steady-state rolling tyre analysis was implemented in order to investigate the effect of tyre normal load, inflation pressure and vehicle manoeuvering behaviour on the contact stress distribution. Al-Qadi and Wang (2009) simulated the interaction of wide-base tyres/pavement and performed an accelerate pavement testing programme to study the fatigue damage on the road caused by dual-tyre assembly. Octahedral shear stress was the key feature in their analysis for comparing the surface cracking in pavements.

In this study, an FE model of a tyre with a tri-axial accelerometer attached to its inner-liner (an intelligent tyre) is developed and the effects of changing the normal load, longitudinal velocity and tyre-road contact friction on the acceleration signal are investigated. In this paper, acceleration signal from a tri-axial accelerometer attached to the tyre inner-liner is used to study the effect of normal load, velocity and friction coefficient on the tyre-pavement interaction, including the contact patch length.

Then, the acceleration responses can be employed The rest of paper is organised as follows; the details of FE models is presented in Section 2, the explanation of experimental test setup is given in Section 3, FE tyre model validation is discussed in Section 4 which is followed by the simulation results, and conclusions in Sections 5 and 6, respectively.

2. FE tyre model

Vulcanised rubber, reinforcing belts and carcase used in tyre structures cause the anisotropic and viscoelastic behaviours under different loading conditions. Figure 1 depicts the complexities associated with reinforcement layers made of steel wires combined with rubber matrix in tyre structures. It is apparent from Figure 1 that a fine mesh is required in the belt region to evaluate the shear stresses between the rebar belt elements. In this paper, a passenger tyre with radius of 300 mm consisted of rubber, carcase, reinforcement layers and belt materials is considered in order to reduce the computational time of the simulation comparing to the complex TBR truck tyre model shown in Figure 1. The hyperelastic, viscoelastic and elastic material properties used in this model are given in Table 1 (Balaramakrishna and Kumar 2009).

The constants used in Yeoh model (given in Table 1) describe the shear behaviour and material compressibility in the strain energy density formulation (Wei and Olatunbosun

$$U = C_{10}(I_1 - 3) + C_{20}(I_1 - 3)^2 + C_{30}(I_1 - 3)^3 + \frac{1}{D_1}(J^{el} - 3)^2 + \frac{1}{D_2}(J^{el} - 3)^4 + \frac{1}{D_3}(J^{el} - 3)^6,$$
 (1)

Table 1. Material types and constitutive models.

Material type	Constitutive model	Model parameters	
Rubber	Hyperelastic (Yeoh Model)	C10	473,685 (N/m ²)
		C20	-119,853 (N/m ²)
		C30	34,293 (N/m ²)
		D1	$5.085 \times 10^{-8} \text{ (m}^2/\text{N)}$
	Viscoelastic(Prony series)	g_i	0.3
		k_i	0
		$ au_i$	0.1 (s)
	Density	μ	1100 (kg/m³)
Belt	Linear elastic	E	172.2×10^9 (Pa)
		ν	0.3
Carcase	Linear elastic	Ε	9.87×10^{9} (Pa)
		ν	0.3

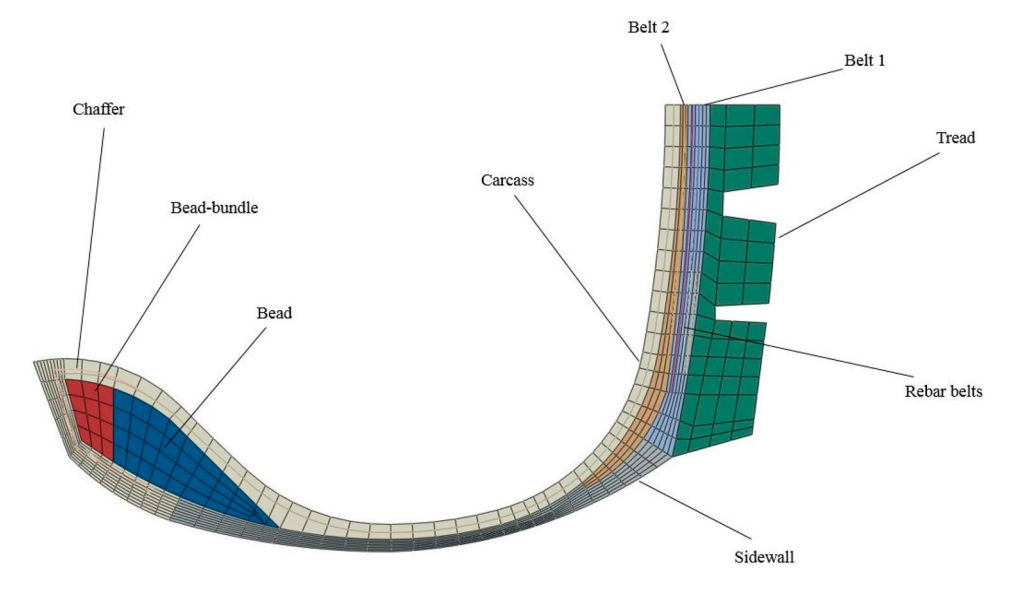


Figure 1. Schematic 2D truck tyre half cross-section sketch and mesh.

where J^{el} is the elastic volume ratio and I_1 is the first deviatoric strain invariant. The viscoelastic material property response is defined in the time domain as follows:

$$g_{\rm R}(t) = 1 - \sum_{i=1}^{N} \bar{g}_i^p (1 - e^{-t/\tau_i^G}),$$
 (2)

where N, \bar{g}_i^p and τ_i^G are the material constants determined by modelling the physical test in ABAQUS.

The following element types (given in the parentheses below) in ABAQUS are implemented in the FE model:

- Modelling pure rubber components: quadrilateral and triangular axisymmetric hybrid elements with twist (CGAX4H and CGAX3H)
- Modelling carcase and belt components: axisymmetric surface elements with twist (SFMGAX1)

The twist option enables the FE model to capture deformations outside the symmetry plane. The modelling procedure in this current framework is followed by four main stages: 2D half axisymmetric, symmetric model generation, reflection of symmetric model and steady-state transport analysis. In the first stage, the 2D tyre half cross-section should be sketched and meshed as shown in Figure 2(a).

Then, it is revolved about its axis of revolution to create the 3D model. The 3D model can be created by symmetric model generation technique. Figure 2(b) shows the 3D passenger tyre model developed, which is obtained from revolving an axisymmetric model about its axis of revolution by implementing the symmetric model generation method in ABAQUS. Segment angles through which the cross-section is revolved and the number of elements used in each segment are defined during the symmetric model generation. The next stage is the reflection of the half tyre model through its symmetry plane in order to create the full tyre model. The reflected model is shown in Figure 2(c). It is worth mentioning that the maximum

shear stress exists between the rebar elements in the belt section (at the belt edge region). Figure 3 shows the high shear stress values at the belt edge region for a tyre with the pressure of 206 KPa.

The loading steps in the tyre model are applied through several stages. In the first simulation (2D axisymmetric model), the inflation pressure of 206 KPa is applied to the inner surface of the 2D axisymmetric model and the results are transferred to the half tyre model. In the second simulation (half tyre model), the footprint solution is obtained over two steps. The prescribed vertical displacement of 20 mm is applied to the road surface in order to model the initial contact between the road and tyre in the first step. In the second step, the displacement boundary condition is removed and the normal load is applied to the road surface reference node and the results are transferred to the next simulation by the symmetric results transfer method in ABAQUS. In the third simulation (full tyre model), the normal load from the previous step is doubled and applied to the road surface reference node. Four different normal loads of 2000, 3000, 4000 and 5000 N are used in the full tyre model.

The last stage of tyre modelling is the steady-state free-rolling analysis where the deformations, stresses, strains, and the footprint shape remain constant over time. When driver changes the velocity and steering wheel angle, the steady state is reached after a few rotations of the tyre. Mixed Eulerian-Lagrangian is used in the steady-state transport analysis in ABAQUS to model rolling and sliding contact of tyre and rigid surfaces. Kinematics of rolling problem is determined in terms of a coordinate frame and the rigid body rotation and deformation are evaluated by Eulerian and Lagrangian methods, respectively. Hence, the time domain is transformed to the purely spatial domain. The effects of normal load, coefficient of friction and velocity on radial acceleration, tangential acceleration and lateral acceleration are studied in the current framework. Three different coefficients of friction are provided for the contact between the tyre and the road surface in this step: 0.4, 0.6 and 0.85. In addition, the values of 30, 50 and

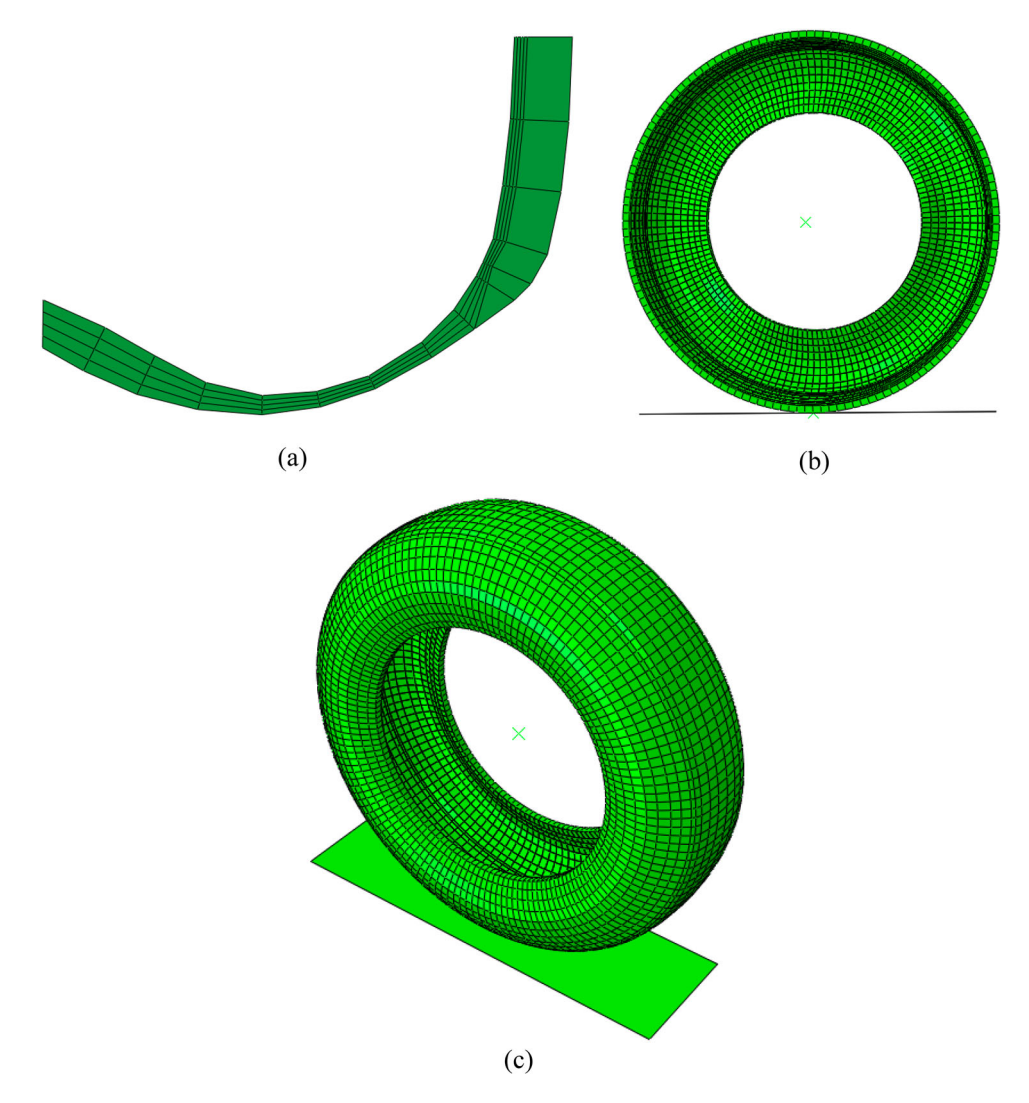


Figure 2. FE model of the intelligent tyre; (a) half cross-section axisymmetric model of tyre, (b) symmetric model generation technique is used to create 3D tyre model from an axisymmetric model and (c) full 3D tyre mesh obtained from the symmetric model generation technique.

70 mph are considered for tyre velocity during the steady-state free-rolling analysis. Figure 4 shows the distribution of acceleration in the 3D tyre model with the velocity of 30 mph, the coefficient of friction of 0.85 and the normal load of 3000 N.

3. Experimental setup

In this study, a tyre testing trailer, which is a quarter car test rig installed in a trailer and towed by a truck, was used. The

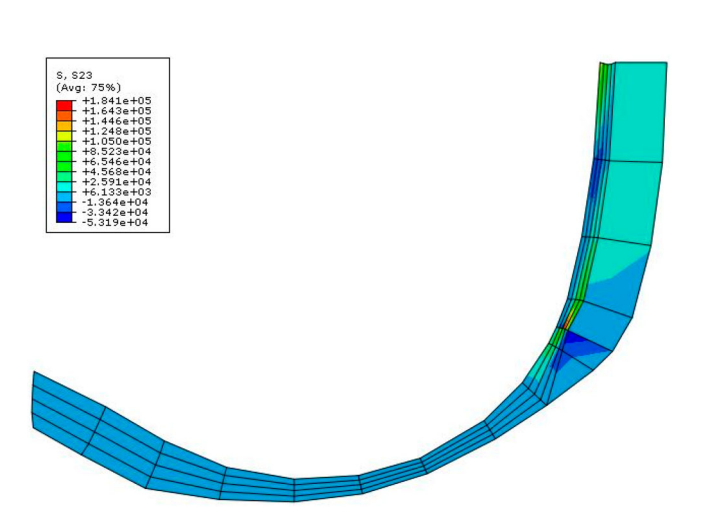


Figure 3. Distribution of shear stress in 2D half tyre model with the pressure of 206 KPa.

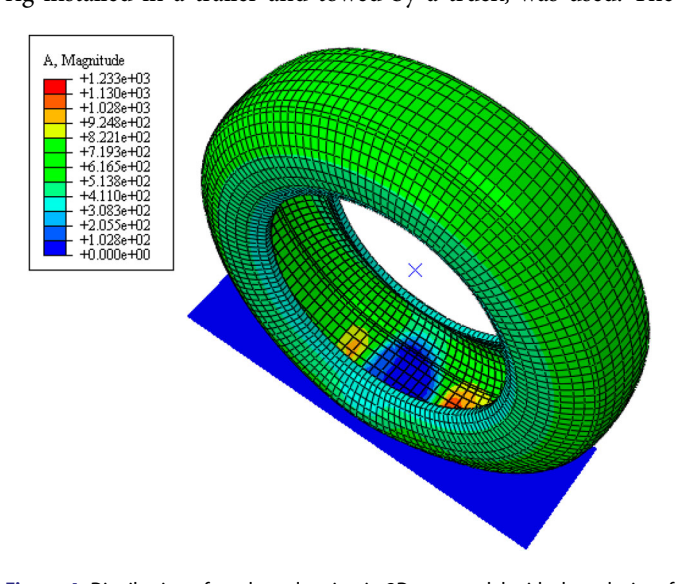


Figure 4. Distribution of total acceleration in 3D tyre model with the velocity of velocity of 30 mph, the coefficient of friction of 0.85 and the normal load of 3000 N.





Figure 5. Trailer test setup.

trailer test setup is shown in Figure 5. There is a water tank-water pump system that provides wet testing condition corresponding to different coefficients of wet surface friction.

The trailer is equipped with different sensors; a six Degrees of Freedom Kistler force hub for measuring the tyre forces and moments, a high resolution encoder (3000 PPR) which was attached to the force hub in order to measure the angular speed of the wheel, VBOX, which is a GPS-based device, used to measure the longitudinal speed of the trailer, and an intelligent tyre, a tyre with tri-axial accelerometer embedded to its inner-liner. The intelligent tyre and the quarter car test rig are shown in Figure 6.

The tyre normal load was controlled using an air spring and a pneumatic pressure transducer, the schematic of normal load control mechanism is shown in Figure 7(a). The maximum load capacity for the normal load controller system (considering the weight of the trailer and air spring and transducer loading capacity) is 10,000 pounds. Also, the wheel slip angle was controlled using a Parker servo motor – motor control system which is shown in Figure 7(b).

A data collecting routine was developed in LABVIEW that collects the time synchronised data of all the sensors with the same sample rate; the sample rate of 1000 Hz was used for this study.

4. FE tyre model validation

Radial and circumferential acceleration signals obtained from the accelerometer, which are attached to the tyre inner-liner, play key roles in estimating the tyre-road contact parameters (Behroozinia et al. 2016b, 2017, 2018a, 2018b). To validate the FE model of the intelligent tyre, a tyre with tri-axial accelerometer was tested with the trailer test setup and the radial and circumferential components of acceleration were compared to the FE tyre model results. The radial and circumferential components of acceleration signal for a complete tyre revolution are shown in Figure 8. It is observed that the trend of signals is the same in both cases of experimental test and FE simulation; however, their magnitudes are different due to using tyres with different dimensions and material properties in experimental test and FE analysis. The trend of the acceleration signals will be used to develop different intelligent tyre-based estimation algorithms. Hence, the purpose was just to see whether the trend of different components of acceleration signals in the FE tyre model is consistent with the experimental data. The amplitude of the signal varies from tyre to tyre based on the tyre size, tyre tread pattern and the tyre compounds; however, the trend of different components of acceleration signal remains constant. Thus, it does not mean that the acceleration signals for different tyres are identical. As it is shown in the following sections, the values of the acceleration responses outside and inside the contact patch area (peak values, and the distance between the peaks in the trend of acceleration responses) change with the tyre types and sizes. In addition, the mesh geometry of tyre in finite element analysis needs to be refined enough due to the interaction of tyre with ground. Thus, the mesh sensitivity analysis using different number of elements is employed to show the maximum Von-Mises stress in Figure 9. The total number of elements used in FE tyre model is 12,097.

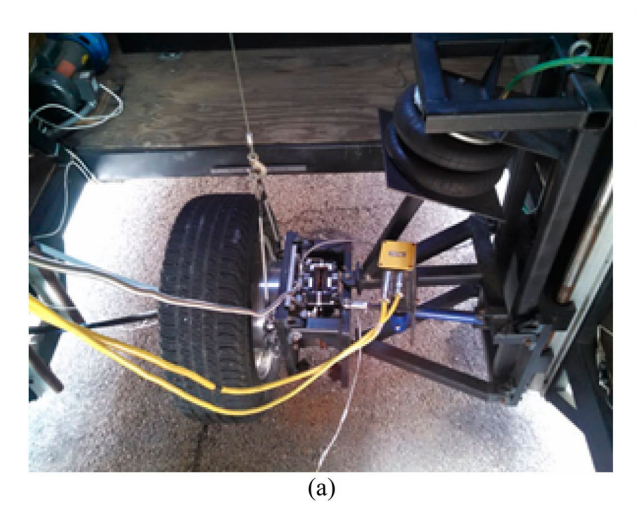




Figure 6. The quarter car test rig: (a) the normal load and slip angle controllers and (b) the tyre with accelerometer embedded to its inner-liner.

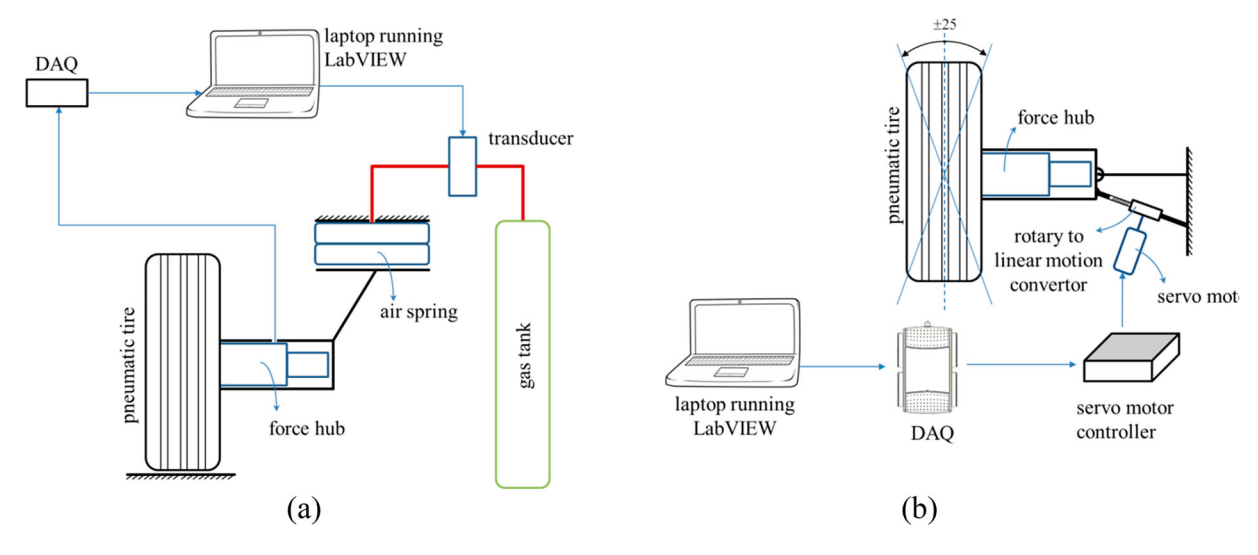


Figure 7. The schematic of trailer's control system: (a) normal load controller and (b) slip angle controller.

5. Results and discussion

In order to investigate the effect of different factors including normal load, surface friction and longitudinal velocity on tyre acceleration, a series of FE analysis were done in ABAQUS

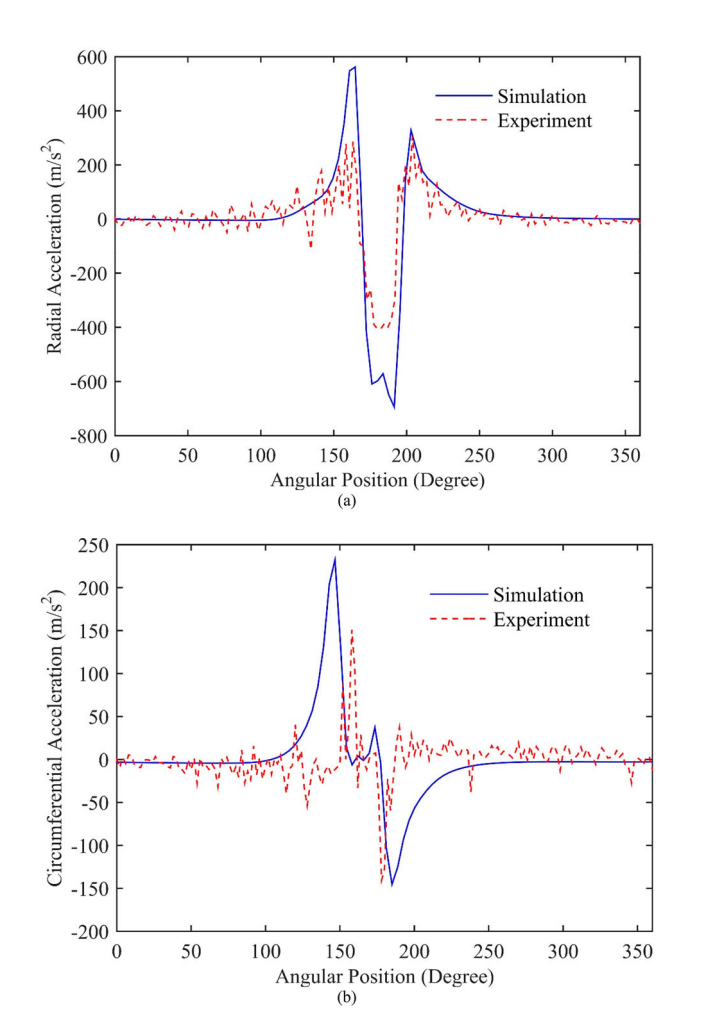


Figure 8. Comparison between the acceleration signals from experimental test setup and FE tyre model: (a) radial and (b) circumferential.

with four normal loads, three longitudinal speeds and three different tyre-road contact frictions.

One of the parameters which can be estimated using intelligent tyre is the contact patch length. The contact patch width is not discussed in this paper since this parameter cannot be estimated using the radial and circumferential components of acceleration signal.

Once the accelerometer goes in and out of the contact patch, two peaks appear in the circumferential and radial components of the acceleration signal (Singh *et al.* 2013, Khaleghian *et al.* 2016). The contact patch length can be calculated as follows:

$$2a = \Delta t_{\rm p}.\nu,\tag{3}$$

where a is half of the contact patch length, $\Delta t_{\rm p}$ is the time difference between acceleration peaks and ν is the longitudinal speed of the wheel. Figures 10 and 11 show the contact patch length for different normal loads calculated from the radial and circumferential components of acceleration signal, respectively.

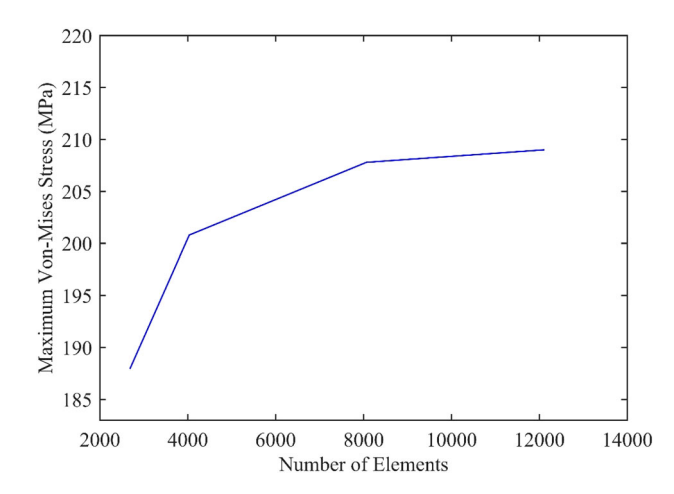


Figure 9. Mesh sensitivity analysis for maximum Von-Mises stress in FE tyre model.

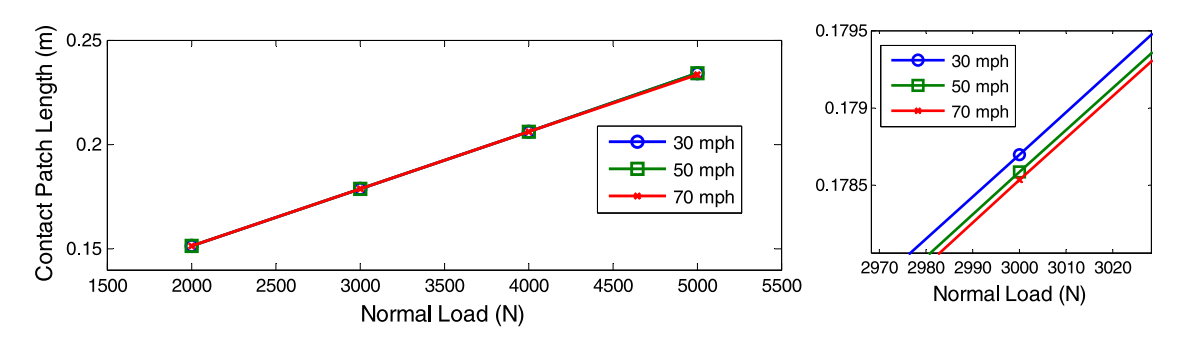


Figure 10. The estimated contact patch length using radial acceleration for the tyre–road contact friction of μ = 0.4.

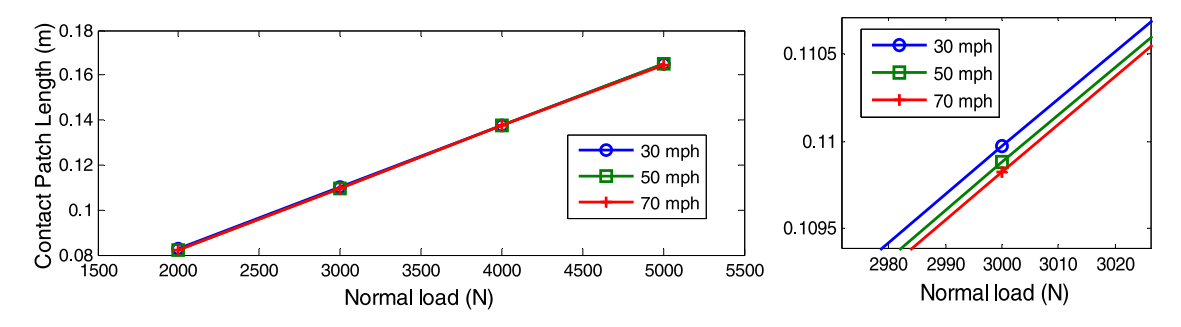


Figure 11. The estimated contact patch length using circumferential acceleration for the tyre–road contact friction of μ = 0.4.

It is observed that the contact patch length estimated using radial component of acceleration signal is larger than that estimated using the circumferential component. Comparing the estimated contact patch lengths from different components of acceleration signals to the actual contact length shown in Figure 12, the one estimated using circumferential acceleration is found to be more accurate. This fact was also shown in literature using experimental data (Khaleghian 2017). Although the

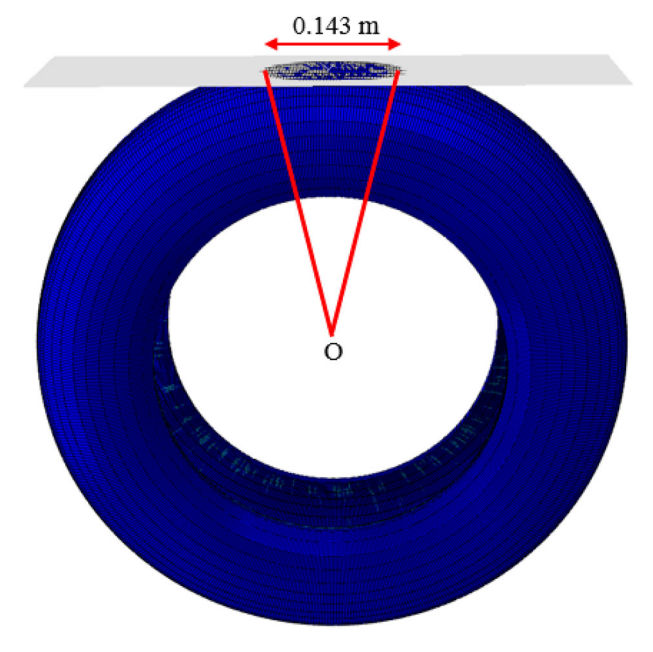


Figure 12. The estimated contact patch length using FE model with friction coefficient of 0.6, velocity of 50 mph and normal load of 4000 N.

radial component of acceleration still can be used to estimate the normal load, it cannot be used to estimate the contact patch length.

It is worth mentioning that the tyre configuration affects the pavement performance since the contact patch area transmits the contact stress between the tyre and pavement (Wang et al. 2012). Additionally, the effect of tyre normal load and friction coefficient is shown in Figure 13. It can be noted that the tyre velocity does not influence the contact pressure distribution in the contact patch area. The contact patch length increases and the projected tyre surface on the pavement approximately becomes rectangular when the tyre normal load increases, as shown in Figure 13.

In addition, longitudinal and transverse contact shear stress distributions in the contact patch area for different cases are shown in Figure 14 in order to investigate the effect of friction coefficient and normal load on the contact shear stresses.

As it is shown in Figure 14, increasing the normal load from 2000 to 4000 lb makes the contact pressure more non-uniform and the maximum value of the contact pressure becomes almost doubled, in spite of an increase in the contact area. Additionally, an increase in the friction coefficient significantly increases the maximum value of the contact pressure and makes the pressure distribution non-uniform.

As it was expected, for specific tyre inflation pressures, higher normal load leads to larger contact patch length. Moreover, when the longitudinal speed of the wheel increases, the contact patch length does not change much. However, contact patch length in higher speed is slightly decreased. The radial and circumferential accelerations for the tyre with different

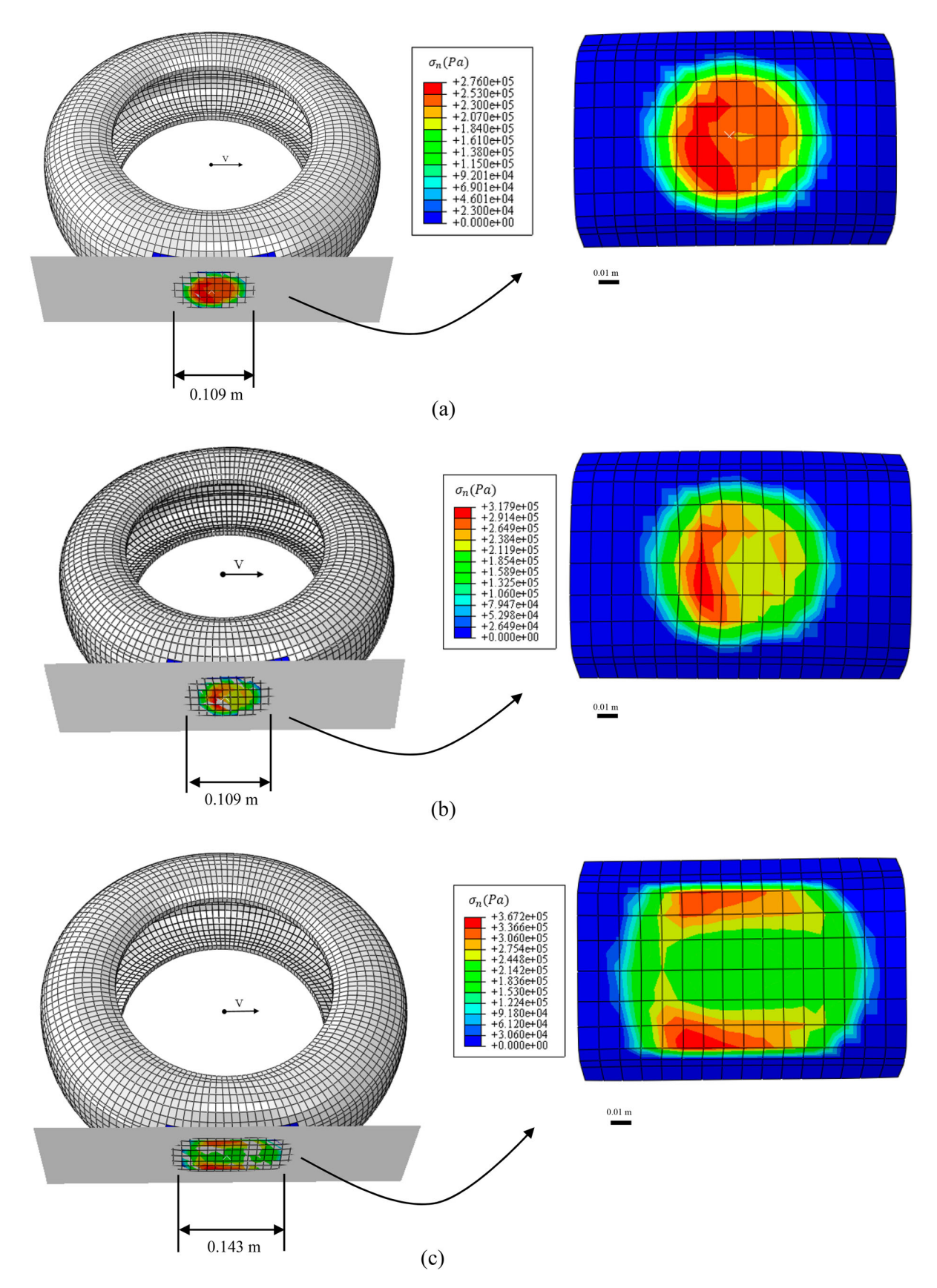


Figure 13. Normal contact pressure distribution in the contact patch area; (a) tyre with the normal load of 2000 N and friction coefficient of 0.4, (b) tyre with the normal load of 2000 N and friction coefficient of 0.85 and (c) tyre with the normal load of 4000 N and friction coefficient of 0.4.

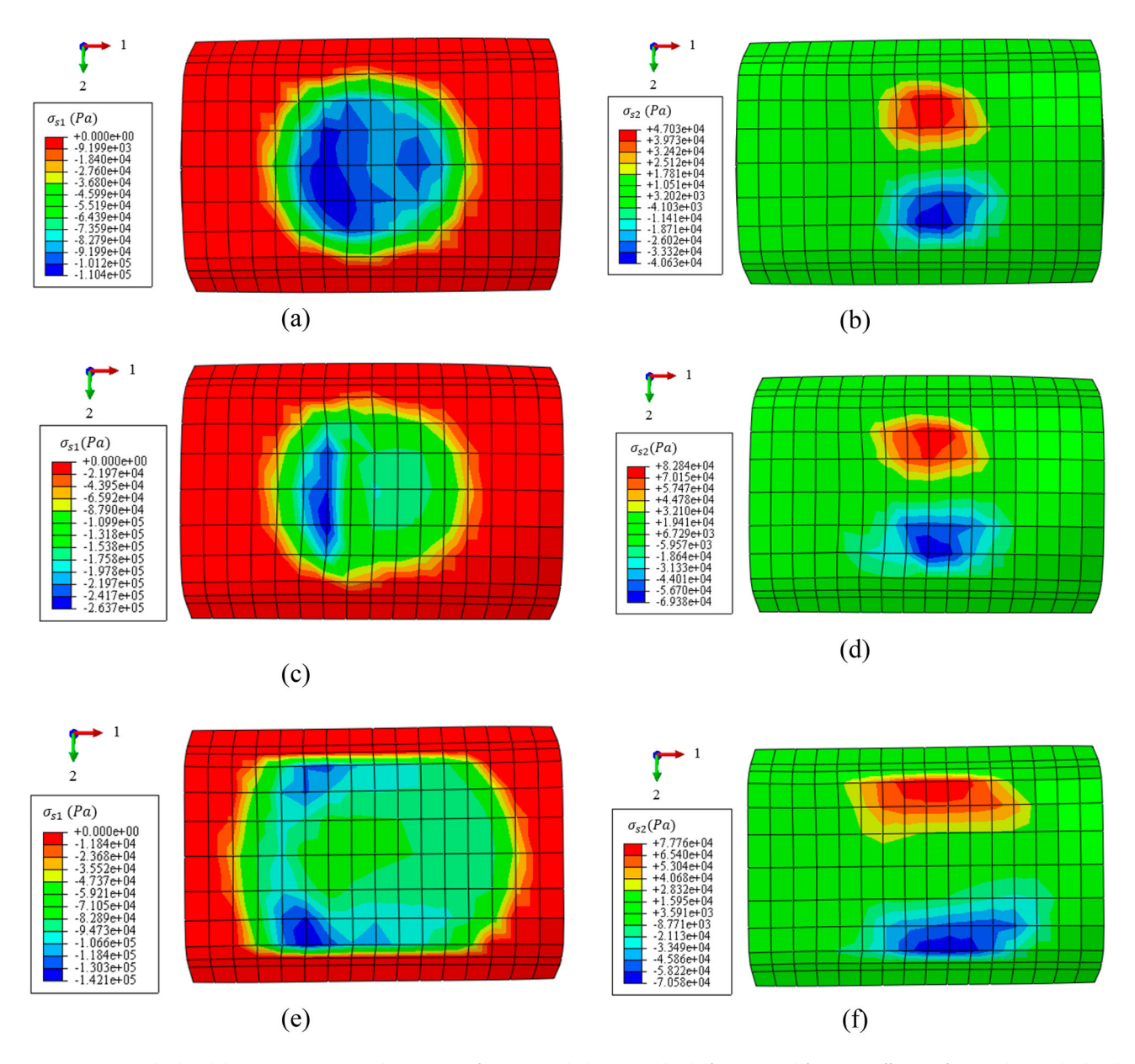


Figure 14. (a) Longitudinal and (b) transverse contact shear stresses for a tyre with the normal load of 2000 N and friction coefficient of 0.4; (c) longitudinal and (d) transverse contact shear stresses for tyre with the normal load of 2000 N and friction coefficient of 0.85; (e) longitudinal and (f) transverse contact shear stresses for a tyre with the normal load of 4000 N and friction coefficient of 0.4.

longitudinal speeds and the normal load of 4000 N are shown in Figures 15 and 16, respectively.

When the wheel speed increases, higher excitation of the tyre in contact area (contact patch) causes the amplitude of tyre acceleration to increase. This phenomenon was seen in all components of acceleration and can be used as a tool to estimate the wheel velocity based on intelligent tyre. Figure 17 depicts the radial and circumferential components of the

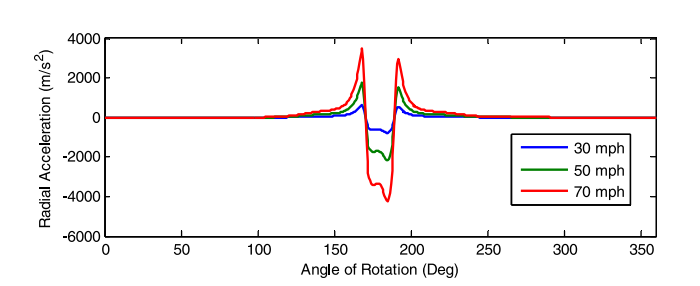


Figure 15. Tyre radial accelerations corresponding to different wheel speeds (μ = 0.85).

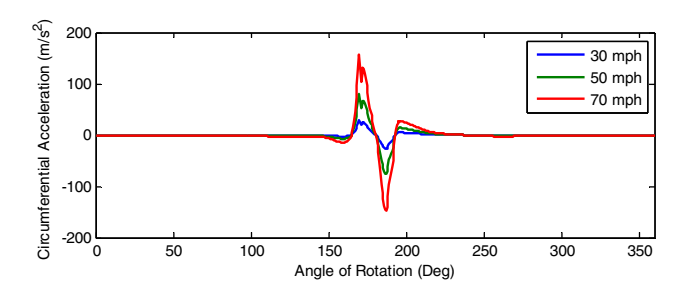


Figure 16. Tyre circumferential accelerations corresponding to different wheel speeds ($\mu = 0.85$).

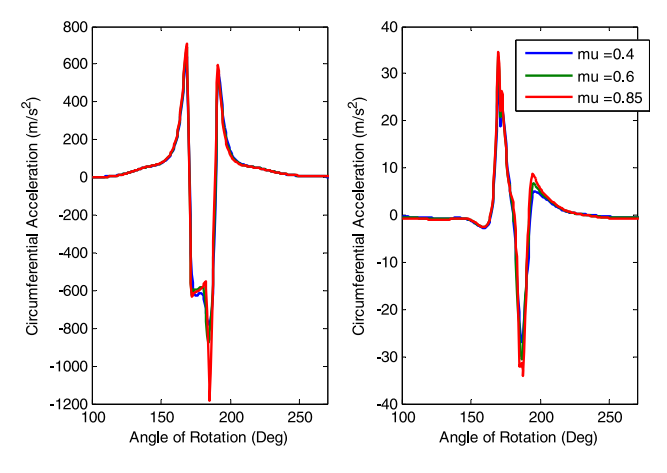


Figure 17. Radial and circumferential components of acceleration for different tyre–road contact coefficients of friction (velocity = 30 mph).

acceleration for the tyre with the normal load of 4000 N and different tyre-road contact coefficients of friction.

Although the tyre–road contact friction seems not to have significant effects on the contact patch length, it is observed that the powers of acceleration signals are different for different tyre–road contact frictions. The energy (power) of a signal x(t) is calculated as follows:

$$E_{\rm sc} = \langle x(t), x(t) \rangle = \int_{-\infty}^{\infty} |x(t)|^2 \mathrm{d}t, \tag{4}$$

$$E_{\rm sd} = \langle x(t), x(t) \rangle = \sum_{-\infty}^{\infty} |x(t)|^2 dt, \tag{5}$$

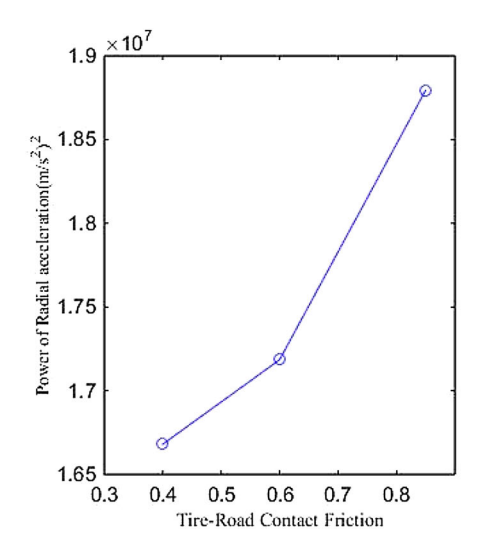
where $E_{\rm sc}$ and $E_{\rm sd}$ are the energy of continuous-time and discrete-time signal x(t), respectively. Figure 18 shows the power of acceleration signals for different contact frictions. This fact can be used to estimate the tyre–road friction using intelligent tyre.

6. Conclusions

Intelligent tyres were introduced as a key to estimate the tyreroad contact parameters by monitoring the interaction between the tyre and the road directly. Accelerometers, piezoelectric strain sensors and pressure sensors are the most common sensors which are used inside the tyre. To develop a comprehensive intelligent tyre-based algorithm, the tyre should be tested under different conditions, which is an expensive and time consuming process.

As the first step of developing such an intelligent tyre algorithm, an FE model of intelligent tyre (a tyre with a tri-axial accelerometer attached to its inner-liner) was developed and the effects of normal load, wheel velocity and tyre-road contact friction on acceleration signal were investigated. The acceleration components obtained from simulation were then compared to the ones collected using experimental trailer test setup and good agreement was observed. Analysing the acceleration signal for different tyre normal load and wheel speed, it was observed that the peaks in circumferential and radial accelerations are correlated to the contact patch length, however using the circumferential acceleration leads to more accurate results. Also, it was found that in the same loading condition, contact patch length slightly decreases once the velocity increases. Furthermore, the effect of normal load and friction coefficient on the contact pressure was studied and it was shown that increasing the normal load and friction coefficient makes the contact pressure more non-uniform and leads to increase the maximum value of the contact

In addition, the simulation results for different longitudinal velocities showed that the amplitude of acceleration signal increases in higher velocities. These facts can be used to develop and intelligent tyre-based algorithm to estimate the wheel velocity and contact patch length. Furthermore, it was observed that the power of acceleration signals is higher on surfaces with higher coefficient of friction. This concept is currently being applied for the estimation of coefficient of friction using the intelligent tyre concept.



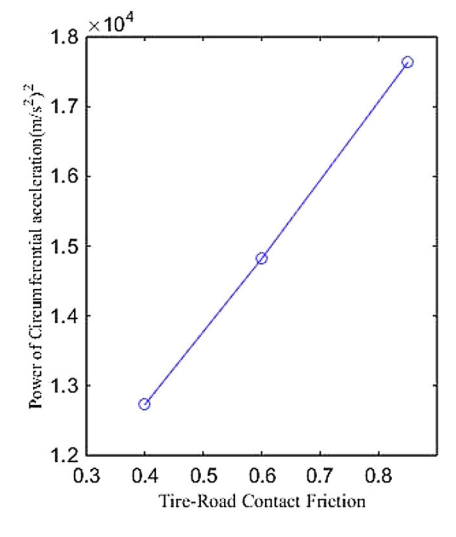


Figure 18. The power of acceleration components in different tyre-road contact friction.



Disclosure statement

No potential conflict of interest was reported by the authors.

References

- Al-Qadi, I.L. and Wang, H., 2009. Full-depth pavement responses under various tire configurations: accelerated pavement testing and finite element modeling. Journal of the Association of Asphalt Paving Technologists, 78, 721-760.
- Bachmann, T., 1995. The importance of the integration of road, tyre and vehicle technologies. PIARC.
- Balaramakrishna, N. and Kumar, R.K., 2009. A study on the estimation of swift model parameters by finite element analysis. Proceedings of the Institution of Mechanical Engineers, Part D: Journal of Automobile Engineering, 223 (10), 1283-1300.
- Behroozinia, P., Bayandor, J., and Mirzaeifar, R., 2016a. Numerical investigation of scale factor in composites applying extended finite element method. AIAA Modeling and Simulation Technologies Conference.
- Behroozinia, P., Mirzaeifar, R., and Taheri, S., 2017a. A review of fatigue and fracture mechanics with a focus on rubber-based materials. Proceedings of the Institution of Mechanical Engineers, Part L: Journal of Materials: Design and Applications.
- Behroozinia, P., Taheri, S., and Mirzaeifar, R., 2016b. Three-dimensional modeling of crack propagation in tires. 190th technical meeting-2016 fall.
- Behroozinia, P., Taheri, S., and Mirzaeifar, R., 2018a. Tire health monitoring using the intelligent tire concept. Structural Health Monitoring.
- Behroozinia, P., Taheri, S., and Mirzaeifar, R., 2018b. An investigation of intelligent tires using multiscale modeling of cord-rubber composites. Mechanics Based Design of Structures and Machines, 46 (2), 168-183.
- Breuer, B., 1992. Measurement of tire-road friction ahead of the car inside the tire. Proceedings of the International Symposium onAdvanced Vehicle Control 1992; AVEC '92, 14-17 September 1992 Yokohama,
- Breuer, B., et al., 2000. The mechatronic vehicle corner of dramstadt university of technology ~ interaction and cooperation of a sensor tire, new low-energy disc brake and smart wheel suspension. (No. 2000-05-0191). SAE Technical Paper.
- Cao, P., et al., 2015. Tire-pavement contact stress with 3D finite-element model—part 2: all-steel tire on heavy vehicles. Journal of Testing and Evaluation, 44 (2), 801-811.
- Cao, P., et al., 2016. Tire-pavement contact stress with 3D finite-element model—part 1: semi-steel radial tires on light vehicles. Journal of Testing and Evaluation, 44 (2), 788-800.
- Cho, J., et al., 2005. Transient dynamic response analysis of 3-D patterned tire rolling over cleat. European Journal of Mechanics-A/Solids, 24 (3), 519-531.
- De Beer, M., et al., 2012. Toward using tire-road contact stresses in pavement design and analysis. Tire Science and Technology, 40 (4), 246-271.
- Ebbott, T., 1996. An application of finite element-based fracture mechanics analysis to cord-rubber structures. Tire Science and Technology, 24 (3), 220-235.
- Eichhorn, U. and Roth, J., 1992. Prediction and monitoring of tyre/road frictioned. XXIV FISITA Congress, 7-11 June, London. Held at the Automotive technology servicing society. Technical papers. Safety, the vehicle and the road. Volume 2 (IMECHE NO C389/321 and FISITA
- Erdogan, G., et al., 2011b. Tire sensors for the measurement of slip angle and friction coefficient and their use in stability control systems. SAE International Journal of Passenger Cars-Mechanical Systems, 4, 44-58.
- Erdogan, G., Alexander, L., and Rajamani, R., 2011a. Estimation of tireroad friction coefficient using a novel wireless piezoelectric tire sensor. IEEE Sensors Journal, 11 (2), 267-279.
- Gent, A.N. and Walter, J.D., 2006. Pneumatic tire.
- Han, Y., et al., 2004. Fatigue life prediction for cord-rubber composite tires using a global-local finite element method. Tire Science and Technology, 32 (1), 23-40.

- Hollingum, J., 2001. Autonomous radio sensor points to new applications. Sensor Review, 21 (2), 104-107.
- Kao, B. and Muthukrishnan, M., 1997. Tire transient analysis with an explicit finite element program. Tire Science and Technology, 25 (4), 230 - 244.
- Kennedy, R. and Padovan, J., 1987. Finite element analysis of a steady-state rotating tire subjected to point load or ground contact. Tire Science and Technology, 15 (4), 243-260.
- Khaleghian, S., 2017. The application of intelligent tires and model based estimation algorithms in tire-road contact characterization. PhD, Virginia Polytechnic Institute and State University, Blacksburg.
- Khaleghian, S., Emami, A., and Taheri, S., 2017. A technical survey on tireroad friction estimation. Friction, 5 (2), 123-146.
- Khaleghian, S., Ghasemalizadeh, O., and Taheri, S., 2016. Estimation of the tire contact patch length and normal load using intelligent tires and its application in small ground robot to estimate the tire-road friction. Tire Science and Technology, 44 (4), 248-261.
- Khaleghian, S. and Taheri, S., 2017. Terrain classification using intelligent tire. Journal of Terramechanics, 71, 15-24.
- Koishi, M., Kabe, K., and Shiratori, M., 1998. Tire cornering simulation using an explicit finite element analysis code. Tire Science and Technology, 26 (2), 109-119.
- Korunović, N., et al., 2011. Finite element analysis of a tire steady rolling on the drum and comparison with experiment. Strojniški vestnik-Journal of Mechanical Engineering, 57 (12), 888-897.
- Matilainen, M.J. and Tuononen, A.J., 2011. Tire friction potential estimation from measured tie rod forces. Intelligent Vehicles Symposium (IV), 2011 IEEE, 320-325.
- Matilainen, M.J. and Tuononen, A.J., 2012. Intelligent tire to measure contact length in dry asphalt and wet concrete conditions. Proceedings of the 11th International Symposium on Advanced Vehicle Control, Seoul, Korea, 9-12.
- Niskanen, A.J. and Tuononen, A.J., 2014a. Three 3-axis accelerometers fixed inside the tyre for studying contact patch deformations in wet conditions. Vehicle System Dynamics, 52 (sup1), 287-298.
- Niskanen, A.J. and Tuononen, A.J., 2014b. Three 3-axis accelerometers on the inner liner of a tyre for finding the tyre-road contact friction indicators. In Proceedings of AVEC International Symposium on Advanced
- Niskanen, A.J. and Tuononen, A.J., 2015. Accelerometer tyre to estimate the aquaplaning state of the tyre-road contact. Intelligent Vehicles Symposium (IV), 2015 IEEE, 343-348.
- Singh, K.B., Arat, M.A., and Taheri, S., 2013. An intelligent tire based tireroad friction estimation technique and adaptive wheel slip controller for antilock brake system. Journal of Dynamic Systems, Measurement, and Control, 135 (3), 031002.
- Tönük, E. and Ünlüsov, Y.S., 2001. Prediction of automobile tire cornering force characteristics by finite element modeling and analysis. Computers & Structures, 79 (13), 1219-1232.
- Wang, H., Al-Qadi, I.L., and Stanciulescu, I., 2012. Simulation of tyrepavement interaction for predicting contact stresses at static and various rolling conditions. International Journal of Pavement Engineering, 13 (4), 310-321.
- Wang, W., Yan, S., and Zhao, S., 2013. Experimental verification and finite element modeling of radial truck tire under static loading. Journal of Reinforced Plastics and Composites, 32 (7), 490-498.
- Wei, C. and Olatunbosun, O.A., 2014. Transient dynamic behaviour of finite element tire traversing obstacles with different heights. Journal of Terramechanics, 56, 1-16.
- Xia, K. and Yang, Y., 2012. Three-dimensional finite element modeling of tire/ground interaction. International Journal for Numerical and Analytical Methods in Geomechanics, 36 (4), 498-516.
- Zang, M., Gao, W., and Lei, Z., 2011. A contact algorithm for 3D discrete and finite element contact problems based on penalty function method. Computational Mechanics, 48 (5), 541-550.
- Zhao, C. and Zang, M., 2014. Analysis of rigid tire traction performance on a sandy soil by 3D finite element-discrete element method. Journal of Terramechanics, 55, 29-37.